Rotational autoionization and energy levels of triplet nf, $v=0$ Rydberg states of H_2

M. D. Lindsay* and F. M. Pipkin†
Lyman Laboratory of Physics, Harvard University, Cambridge, Massachusetts 02138
(Received 5 June 1996; revised manuscript received 23 August 1996)

We have measured the energy levels and purely rotational autoionization rates of 25 different triplet Rydberg states of the H_2 molecule with quantum numbers $n=14$–29, $L=3$, $v=0$, and $R=2$–4. Electron impact excites the ground-state molecules in a beam to the metastable $c(2p)\ ^3\Pi_u$ states. Two-color laser excitation from two counterpropagating single-mode cw dye laser beams excites the metastable molecules through an intermediate $(3d)\ ^3\Sigma$ or $(3d)\ ^3\Pi$ state to the triplet nf Rydberg states. The linewidths of the transitions to the Rydberg states give the autoionization rates, which vary widely and agree satisfactorily with the quadrupole-moment-polarizability long-range Coulomb interaction model. The laser transitions have been measured to 0.002 cm^{-1}. We use these measurements, the model, and an extrapolation of the Rydberg series to derive the ionization potential of the metastable $c(2p)\ ^3\Pi_u\ v=0$ states with an accuracy of 0.020 cm^{-1} and the energy difference between the singlet ground state and the triplet metastable $c(2p)\ ^3\Pi_u$ states with an accuracy of 0.025 cm^{-1}. This allows the whole singlet and triplet manifolds of H_2 to be linked together with higher accuracy: our correction to Dieke's H_2 triplet term values is $-149.704(25)$ cm^{-1}. [S1050-2947(97)00202-3]

PACS number(s): 33.80.Eh, 33.80.Rv, 33.70.Jg

I. INTRODUCTION

The Rydberg states described in this paper are interesting because their decay dynamics are strongly influenced by the H_2^+ core and their energy levels show an easily calculable shift from H atom energy levels. For the Rydberg states described in this paper and in Refs. [1,2], the dominant decay mode is autoionization, in which the vibrational and/or rotational energy of the H_2^+ core transfers to the Rydberg electron whose electronic energy is already very close to the ionization potential. The extra energy ejects the outer electron at a rate given by Fermi's golden rule. The energy levels are perturbed from H atom energy levels and the shifts can be calculated using perturbation theory. This long-range Coulomb multipole moment model of the interaction between the H_2^+ core and the Rydberg electron (the long-range model), giving the autoionization rate and energy-level-shift calculations, is presented in detail in Ref. [3]. Extrapolating our measured series of triplet Rydberg states to the ionization limit where the singlet and triplet manifolds merge provides a highly precise link between the two separate manifolds of states.

The Rydberg H_2 states described in Ref. [1] were $v=1$ states, with $R=0$–4. (v is the vibrational quantum number of the H_2^+ core and R is its rotational quantum number.) Since a vibrational quantum of energy for H_2^+ is about 40 times the rotational quantum of energy, most of the energy for autoionization of $v=1$ states comes from the vibrational motion of the core. Thus purely rotational autoionization, the subject of this paper, for which the core quantum numbers are $v=0$, $R=1,2,3,4,...$, is in a different dynamical regime. More of the purely rotationally autoionizing states measured in this paper are higher in R than the states measured in Ref. [1] because higher R values are necessary to achieve the energy needed for autoionization, when $v=0$. A higher R for a state means that more decay channels are accessible, which might lead to differences in dynamical behavior.

The Introduction of Ref. [1] contains a limited review of spectroscopic work done on Rydberg hydrogen up to about 1989. Since then, much more work has been done. Jungen *et al.* [4] have done extensive Fourier spectroscopy measurements of the energy levels of H_2 and D_2. They studied a very wide range of states, both singlet and triplet, for several values of L, with an energy resolution of 0.05 cm^{-1}. Their work remains the most accurate study of D_2. This paper reports energy-level measurements of a relatively small number of $v=0$ H_2 states, accurate to 0.025 cm^{-1}. The $v=0$, $R=3$ energy level of the H_2^+ ion core has been measured to high accuracy using the Rydberg electron as a probe of the core [5]. The long-range Coulomb model has been extended and used to determine ir spectra of H_2 and D_2 [6]. An extensive series of high-L microwave transitions in Rydberg H_2 has allowed determination of the Q and α of the H_2^+ core [7]. More recent highly accurate measurements in singlet H_2 have given an updated value for the ionization potential (V_{ion}) of H_2, as well as HD and D_2 [8,9]. Interactions between Rydberg series of different v and R have been studied [10]. The autoionization rates and energy levels of triplet nf Rydberg states of HD, with a permanent dipole moment in the core, have been studied [11].

This paper reports measurements of the autoionization rates and energy levels of a variety of triplet Rydberg states of H_2 with quantum numbers $n=14$–29, $L=3$, $v=0$, $R=2$–4, and $N=1$–4 [2]. The actual measurements are of linewidths of transitions to the Rydberg states and of the energies of those laser transitions from low-lying $2p\ ^3\Pi$, $v=0$ metastable states of H_2, through several triplet $v=0$ intermediate states. The Lorentzian linewidths directly yield the autoionization decay rates of the Rydberg states. Energy levels (term values) of the Rydberg states are obtained from the transition energies by extrapolating the Rydberg series and

*Present address: Physics Department, University of Louisville, Louisville, KY 40292.
†Deceased.

by using the measurement of the ionization potential of H_2 [12,8,9] to link the triplet states to the V_{ion} and to the (singlet) ground state, as described in Refs. [1,2]. This gives the absolute energy levels of all of the measured $2p$, $3d$, and nf triplet states, even though no direct transition is measured between them and the ground state.

These are, to our knowledge, the first quantitative measurements of purely rotational autoionization rates of nonpenetrating high-n and high-L Rydberg states of triplet H_2. The rates are compared with the theoretical predictions of Ref. [3]. The energy levels of $v=0$ Rydberg states are found relative to the metastable $c(2p)\ ^3\Pi_u$, $v=0$ states to an accuracy of 0.003 cm^{-1}. The absolute energy levels of the $2p\ ^3\Pi_u$, $v=0$ states are found to an accuracy of 0.025 cm^{-1}, linking the singlet and triplet manifolds with high precision. All errors and values in parentheses are one standard deviation error.

II. SUMMARY OF EXPERIMENTAL PROCEDURE

This paper follows the notation used by Hougen [13] and by Refs. [1,2]. n is the principal quantum number of the outer electron, analogous to n for the H atom. L is the orbital angular momentum of the outer electron, also analogous to the H atom. v is the vibration of the two protons and R is the rotation of them. N is the total angular momentum of the molecule excluding spins. For the Rydberg H_2 molecules $N=L+R$. The Rydberg nf states are in Hund's coupling case d, the lower-lying $2p$ states are in Hund's case b, and the $3d$ states are intermediate between cases b and d.

The experimental method for the measurements reported in this paper is the same as that described in detail in Refs. [1,2]. Those papers contain schematics of the apparatus used for this experiment. Briefly, we use a molecular beam in a high vacuum so that the Rydberg molecules do not collide while they are being measured. We start with ground-state H_2 and bombard it with 18-eV electrons in a narrow slit in the vacuum chamber. There the H_2 is collisionally excited into a multitude of states, including the metastable $2p\ ^3\Pi_u$, $v=0$ states [14]. The excited molecules travel 20 cm through the vacuum chamber, during which time almost all of the excited states, except the metastable states, decay back to the ground state. We use two separate cw single-frequency dye laser systems, each with a bandwidth of about 20 MHz, to excite the $2p$ molecules to the Rydberg states. The first laser selectively excites the $2p$ molecules to a particular $3d$ state. Then the second laser immediately and selectively excites the $3d$ molecules to an nf triplet Rydberg state. The two lasers are lined up to be collinear and counterpropagating. The excitation to the $3d$ states is monitored by a uv photomultiplier tube, which detects the continuum of uv light emitted by the $3d$ state as it decays. The excitation to the Rydberg states is monitored by a channeltron in an electron lens arrangement. The H_2^+ ions produced by the autoionizing states are detected.

Transition identification is made by correspondence with the predicted positions of the transitions, as calculated by the model of Ref. [3]. Also essential for planning the measurements and finding transitions were the tables of H_2 transitions and energy levels of Dieke, as compiled by Crosswhite [15].

III. LINE-SHAPE ANALYSIS AND AUTOIONIZATION RATE DISCUSSION

During an autoionization rate measurement the laser exciting the $3d$ state was fixed and the second laser was scanned across the transition to the Rydberg state. The channeltron output, the second laser's power level, and reference étalon fringes were recorded by a computer. The digitized line shapes were numerically fit to a Voigt profile model and the true Lorentzian widths were extracted. The autoionization rate is simply 2π(width). The exact correspondence between Voigt profile widths and true Lorentzian widths depends nonlinearly on the Lorentzian width and is described in Ref. [1]. We measured the Gaussian component of the Voigt profiles to be 60 ± 10 MHz. True Lorentzian widths ranged from 15 to 559 MHz. The errors in the widths come from the standard deviation of the widths from several different scans over the same transition. Special care was taken to be sure that the transitions to the Rydberg states ($nf\leftarrow3d$) were not saturated. We also repeatedly sprayed the inside of the vacuum chamber surrounding the laser–molecular-beam interaction region with graphite powder to reduce stray static electric fields.

The multiple overlapping lines in one scan of one transition are due to fine structure. Each fine-structure component has the same width, but a different strength. When the splitting is greater than or on the order of the autoionization width, the true width is extracted by fitting the line shape to a sum of lines, each with a different center position. For a particular Rydberg state, the widths of the components, although allowed to vary freely in the least-squares fit, were always within 20% of each other. We ignored any broadening that might be due to fine-structure splitting much less that the autoionization width. This is justified since the fine-structure component with highest J is expected to be much more intense (by at least a factor 5) than the components with lower J very close in energy to it. (This has been verified with measurements of completely resolved and assigned fine-structure components of other states of H_2 [16,17].)

Typical transitions are shown in Fig. 1. The smooth line through the measured line profile is the fit to the sum of Lorentzians. The horizontal axis is the offset from the peak of the line, in megahertz. We obtained this local scaling from the 299.975-MHz étalon fringes that were taken simultaneously with the line profile. The vertical axis is scaled in arbitrary linear units; the zero of the vertical axis corresponds to the true signal plus noise zero.

Table I lists the nf, $v=0$ Rydberg levels observed, and in the second column their measured true Lorentzian width and one standard deviation error of each measurement. The third column is the theoretical prediction for the Lorentzian width derived from the autoionization rate prediction of Ref. [3]. Column 4 compares the measurements with theory, in terms of experimental error. In general, for states for which there is a theoretical prediction [3], agreement is satisfactory. The majority of measured widths tend to be a little larger than the theoretical values, especially for the narrower states. This is most likely due to residual weak unresolved fine-structure components very close to the main component.

The groupings by N, with other quantum numbers held constant, allow one to see the autoionization rate's strong

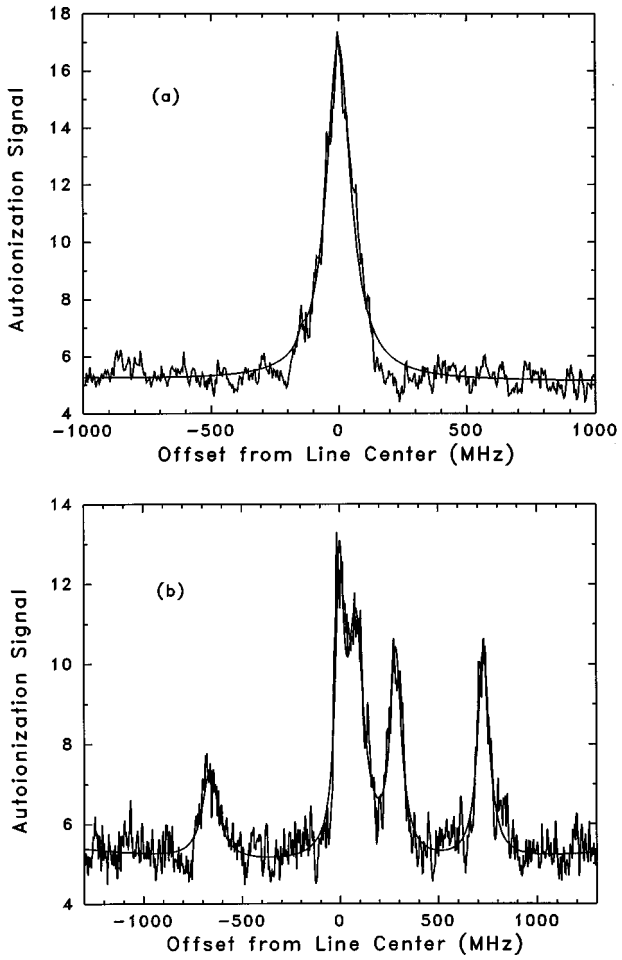

FIG. 1. Typical line profiles acquired while scanning the ir laser over transitions from the intermediate states to the Rydberg states. The smooth line is the sum of Lorentzians fit, which gives the Lorentzian width and autoionization rate of the Rydberg state, as described in the text. (a) is the para transition $15f$, $v=0$, $R=4$, $N=3\leftarrow 3d\ ^3\Pi$, $v=0$, $N=3$ (p. 69 of Ref. [2]). This transition must occur by the $\Delta R=-4$ process as there is not enough energy to autoionize if $\Delta R=-2$ (marked NA in text). Nevertheless, it is fairly strong and wide. (b) is the ortho transition $20f$, $v=0$, $R=3$, $N=1\leftarrow 3d\ ^3\Pi$, $v=0$, $N=3$ (p. 62 of Ref. [2]). Spectra of all other lines tabulated are in Ref. [2].

dependence on N. For example, in the trio of states nf, $v=0$, $R=3$, $N=3,2,1$, where $n=20,21,22$, the measured and predicted autoionization rates go down by more than an order of magnitude as N goes from 3 to 1.

Other decay modes of the Rydberg H_2 molecules might broaden the lines if the rates for the other processes were on the order of or larger than the autoionization rate of about $10^9\ s^{-1}$. For $L=3$ Rydberg states in the range $n=10$–30, the radiative decay rate is about $10^6\ s^{-1}$, three orders of magnitude smaller than our measured autoionization rates, thus radiative decay has no measurable effect in our experiment. There is no evidence that any other decay processes spuriously broaden our lines. There is no transit time broadening since the transit time through the apparatus is much larger than the autoionization time. The good agreement of linewidth with prediction indicates that the dominant mode of decay for the Rydberg states measured is rotational autoionization.

TABLE I. Autoionization widths of Rydberg states, compared with the theoretical predictions of the long-range model. NA (not allowed) indicates that the state has too little core energy for $\Delta R=-2$ autoionization, so the long-range model predicts that autoionization will not occur, given its approximations. BT (below threshold) indicates that the state apparently has too little core energy for any autoionization to occur. See Sec. III for a discussion.

Rydberg state label nf, v, R, N	Expt. width (MHz)	Theor. width (MHz)	Difference (Expt.)−(Theor.) / (error)
$2p\ ^3\Pi$, $v=0$, $N=2\rightarrow 3d\ ^3\Sigma$, $v=0$, $N=2\rightarrow$			
$25f$, 0, 2, 2	35(16)	BT	
$26f$, 0, 2, 2	61(21)	NA	
$25f$, 0, 2, 3	204(86)	BT	
$26f$, 0, 2, 3	162(77)	234	−0.9
$2p\ ^3\Pi$, $v=0$, $N=2\rightarrow 3d\ ^3\Pi$, $v=0$, $N=3\rightarrow$			
$25f$, 0, 2, 4	411(93)	BT	
$26f$, 0, 2, 4	143(13)	NA	
$27f$, 0, 2, 4	273(50)	NA	
$28f$, 0, 2, 4	559(34)	NA	
$29f$, 0, 2, 4	533(219)	NA	
$2p\ ^3\Pi$, $v=0$, $N=1\rightarrow 3d\ ^3\Pi$, $v=0$, $N=2\rightarrow$			
$20f$, 0, 3, 1	21(16)	8	0.8
$21f$, 0, 3, 1	18(19)	7	0.6
$22f$, 0, 3, 1	19(25)	6	0.5
$20f$, 0, 3, 2	133(29)	109	0.8
$21f$, 0, 3, 2	154(27)	94	2.2
$22f$, 0, 3, 2	148(40)	82	1.6
$20f$, 0, 3, 3	320(52)	333	−0.3
$21f$, 0, 3, 3	491(50)	286	4.1
$22f$, 0, 3, 3	267(137)	250	0.1
$2p\ ^3\Pi$, $v=0$, $N=2\rightarrow 3d\ ^3\Pi$, $v=0$, $N=3\rightarrow$			
$17f$, 0, 4, 2	179(69)	141	0.6
$18f$, 0, 4, 2	139(26)	119	0.8
$19f$, 0, 4, 2	197(30)	101	3.2
$14f$, 0, 4, 3	<15(11)	NA	
$15f$, 0, 4, 3	103(11)	NA	
$16f$, 0, 4, 3[a]	45(16)	NA	
$17f$, 0, 4, 3	429(57)	385	0.8
$18f$, 0, 4, 3	339(61)	325	0.2

[a]Perturbed state for which the long-range model may not be valid.

A. Not allowed (NA) states

One interesting feature of the states we measured is that several have no theoretical prediction for their autoionization rate. These are marked with NA (not allowed) or BT (below threshold) in Table I. This indicates that according to the long-range model developed in Ref. [3], the states should not autoionize. The model only allows $\Delta R=-2$ autoionization, due to the interactions of the Rydberg electron and the quadrupole moment and polarizability of the H_2^+ core. Of course the core has higher-order moments that could allow $\Delta R=-4$ or more autoionizations, but the theory does not account for these processes. $\Delta R=-2$ autoionization is forbidden for the three $R=4$ states at the bottom of Table I marked NA, due to energy conservation: if the core loses only its third and

fourth quanta of rotational excitation, the Rydberg electron would not gain enough energy to ionize. (However, if $\Delta R=-4$ the three states could autoionize.) This causes the long-range model to predict zero autoionization rate. Thus these $R=4$ states most likely are undergoing $\Delta R=-4$ autoionization via the rotating H_2^+ core's octopole moment and quadrupole polarizability. This higher-order process is expected to be quite slow and in fact the lines corresponding to transitions to those states are the narrowest we have measured. The actual measured widths of the lines were almost entirely the Gaussian instrumental width. Nevertheless, the lines' signal strength was reasonably large.

The $26f$, $v=0$, $R=2$, $N=2$ state and the $26f-29f$, $v=0$, $R=2$, $N=4$ states marked NA at the top of Table I are in the NA category for another reason. For these states, if the H_2^+ core lost its two quanta of rotational energy, the Rydberg electron would have enough energy to autoionize. However, the autoionization selection rules $\Delta L=0$ and $\Delta N=0$, combined with $N=R+L$, means that R cannot go to zero given the starting values of $L=3$, $N=2$ or 4. Once again the model indicates this by predicting no autoionization, within its approximations. The observed autoionization of these states can be explained by higher-order $\Delta R=-2$ autoionization decay processes that do allow N to change by one in the decay. It may reflect the fact that L, R, and N are not rigorously perfect quantum numbers or it may reflect the mechanism describe below for BT states. These NA states also have fairly strong signals, approximately as strong as the other, allowed, transitions.

B. Below threshold (BT) states

The states marked BT in Table I offer yet another scenario. For these states, even if the H_2^+ core gives up all its rotational energy, the Rydberg electron will still not have enough energy to autoionize. Thus it appears that energy conservation forbids any autoionization by any order process. However, some of the BT lines are quite strong, as strong as the above threshold, allowed lines. Also some of the BT lines were quite narrow as one would expect for a slow process, but some were wide, as well as strong, e.g., the $25f$, $v=0$, $R=2$, $N=4$ line. ''Forced ionization'' [18–20], also known as core-assisted field ionization, is responsible for the ionization of these states marked BT. It is well known that highly excited Rydberg atoms or molecules can be field ionized by an external static electric field. The threshold external field F_{thresh} at which field ionization starts to occur is given approximately by [21]

$$F_{\text{thresh}}=\frac{1}{16n^4}, \tag{1}$$

where F is in atomic units of 5.1×10^9 V/cm. In the canonical system of an H atom, $-\mathcal{R}/n^2$ is the true total energy of the Rydberg electron. In our system of autoionizing Rydberg H_2 the Rydberg electron also has the H_2^+ core energy $E(R)$ available to it. If this energy is counted, the total energy of the Rydberg electron is $-\mathcal{R}/n^2+E(R)$. This extra energy $E(R)$ can be thought of as depressing the ionization potential by an amount $E(R)$ and reducing F_{thresh} below that given in Eq. (1), allowing field ionization to occur more easily, at a lower external field. The new lower electric field F_{thresh} in the presence of core excitation energy $E(R)>0$ is

$$F_{\text{thresh}}=\frac{\left(E(R)-\frac{1}{2n^2}\right)^2}{4}. \tag{2}$$

For $n=25$ and $E(R=2)=174.23$ cm^{-1}, the threshold electric field for field ionization over the depressed ionization potential is only 0.045 V/cm, which could easily be obtained from stray static electric fields in the laser–molecular-beam interaction region. As shown in Sec. IV, each BT molecular state's total energy is only about 1 cm^{-1} below the ionization potential. In these cases, a very weak electric field is enough to tear off the Rydberg electron of the H_2 *molecule* with core excitation, even though a relatively strong field of about 820 V/cm would be required to field ionize an $n=25$ H *atom*.

IV. ENERGY-LEVEL ANALYSIS AND DISCUSSION

Transition energy measurements were made by fixing the lasers to the peaks of their transitions. The energies of the beams were measured with I_2 lines [22,23] and with a wavemeter [24]. The wavemeter measured the laser frequencies with an accuracy of 0.002 cm^{-1}. The absolute energy levels of the nf states were found using a method described in more detail in Ref. [1]. Briefly, this involved finding the ionization potential $V_{\text{ion}}(2p)$ of $2p$ states using the measurements of the transitions that came from that $2p$ state. The rotational energy of the H_2^+ core $E(R)$ [25,26,5] and the energy shift $E_{\text{quad,pol}}$ from H atom levels due to the H_2^+ core provided by the long-range model of Ref. [3] were also needed. Figure 2 shows the energy levels. We have

$$V_{\text{ion}}(2p)=\Delta E(3d\leftarrow 2p)+\Delta E(nf\leftarrow 3d)+\mathcal{R}(H_2)/n^2 - E(R)-E_{\text{quad,pol}}, \tag{3}$$

where $\Delta E(b\leftarrow a)$ is the measured transition energy between states a and b. Tables II and III give the $E(R)$ and $E_{\text{quad,pol}}$ values used in this paper. $\mathcal{R}(H_2)$ is the Rydberg constant for H_2^+ and e^-, 109 707.4496 cm^{-1}. Using Eq. (3), each different nf state gave a slightly different value for $V_{\text{ion}}(2p)$. All of the values of $V_{\text{ion}}(2p)$ related to a particular $2p$ state were averaged; this amounts to an extrapolation of the Rydberg series. The typical scatter in the individual values of $V_{\text{ion}}(2p)$ is about 0.02 cm^{-1}. This is indicative of the error in $E_{\text{quad,pol}}$ since all the other terms in Eq. (3) have much smaller errors. (The $16f$, $v=0$, $R=4$, $N=3$ state is clearly perturbed and was excluded from all analysis.)

The interval $\Delta E(2p\leftarrow X)$ between the triplet $2p$ states and the (singlet) ground state X (which is not directly measured) is of course

$$\Delta E(2p\leftarrow X)=V_{\text{ion}}(H_2)-V_{\text{ion}}(2p). \tag{4}$$

$V_{\text{ion}}(H_2)$, the ionization potential of H_2, is given as $124\,417.507\pm0.012$ cm^{-1} by a separate experiment [8,9]. The absolute energy levels of the $3d$ and nf states can be found by adding their respective transition energies to $\Delta E(2p\leftarrow X)$. The error in $\Delta E(2p\leftarrow X)$ is 0.025 cm^{-1}, approximately the sum in quadrature of the errors of the right-

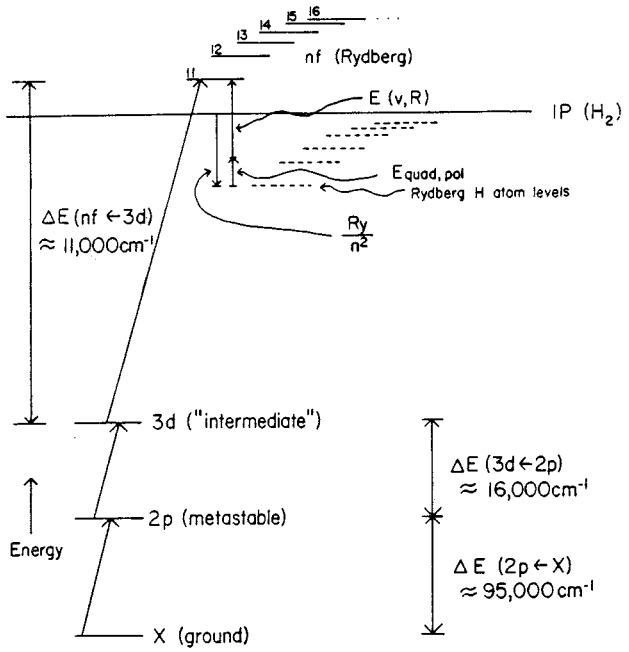

FIG. 2. Energy-level scheme for experiment. Laser excitations are $2p$ to $3d$ and $3d$ to nf. The autoionizing Rydberg series states above the ionization potential are the ones to which transitions are measured. The dotted line Rydberg series states just below the ionization potential are the H atom Rydberg levels, which must be corrected by the H_2^+ core energy $E(v=0,R)$ and the long-range Coulomb perturbation $E_{\mathrm{quad,pol}}$ to get actual H_2 energies. This diagram is not to scale vertically.

hand side of Eq. (4). This is also the error for all of the triplet energy levels since the transition frequency errors for $\Delta E(3d \leftarrow 2p)$ and $\Delta E(nf \leftarrow 3d)$, 0.002 cm^{-1}, are much smaller than 0.025 cm^{-1}.

The transition frequencies we measured are listed in Tables IV and V. Table IV gives the frequencies of transitions between $2p$ states and $3d$ states, $\Delta E(3d \leftarrow 2p)$. Measurements of these intervals were essential in locating and calculating the absolute energy levels of the Rydberg states, which are discussed in the rest of this section. Of the eight $3d \leftarrow 2p$ transitions measured, we only used the second, fourth, and fifth transitions to obtain Rydberg states.

Table V gives the frequencies of transitions between the $3d$ states and the nf Rydberg states, $\Delta E(nf \leftarrow 3d)$. For all transition measurements in both tables, the lasers were set to the peaks of the transitions. This corresponds to transitions from the lower state's spin sublevel of maximum J to the upper state's spin sublevel of maximum J.

TABLE II. Rotational energy levels of H_2^+ core, taken or extrapolated from Refs. [25,5].

R	Energy level $E(R)$ (cm^{-1})
0	0
1	58.2322(20)
2	174.2323(20)
3	347.0912(20)
4	575.4503(80)

TABLE III. Energy correction to the Rydberg electron energy due to the long-range influence of the H_2^+ core. $E_{\mathrm{quad,pol}} = E^{(1)}_{\mathrm{quad}} + E^{(1)}_{\mathrm{pol}} + E^{(2)}_{\mathrm{quad,pol}}$.

Rydberg state label nL, v, R, N	$E^{(1)}_{\mathrm{quad}}$	$E^{(1)}_{\mathrm{pol}}$	$E^{(2)}_{\mathrm{quad,pol}}$
25f, 0, 2, 2	−0.0315	−0.0743	0.0021
26f, 0, 2, 2	−0.0280	−0.0661	−0.0015
25f, 0, 2, 3	0.0578	−0.0646	0.0075
26f, 0, 2, 3	0.0514	−0.0575	−0.0042
25f, 0, 2, 4	0.0789	−0.0623	−0.0022
26f, 0, 2, 4	0.0701	−0.0554	−0.0186
27f, 0, 2, 4	0.0626	−0.0495	0.0099
28f, 0, 2, 4	0.0561	−0.0444	0.0042
29f, 0, 2, 4	0.0505	−0.0400	0.0025
20f, 0, 3, 1	−0.2172	−0.1629	0.0149
20f, 0, 3, 2	−0.0917	−0.1492	0.0085
20f, 0, 3, 3	0.0483	−0.1339	0.0082
21f, 0, 3, 1	−0.1876	−0.1409	0.0132
21f, 0, 3, 2	−0.0792	−0.1290	0.0155
21f, 0, 3, 3	0.0417	−0.1158	0.0392
22 f, 0, 3, 1	−0.1632	−0.1226	0.0118
22 f, 0, 3, 2	−0.0689	−0.1123	0.0075
22 f, 0, 3, 3	0.0363	−0.1008	0.0100
17f, 0, 4, 2	−0.2550	−0.2565	0.0185
18f, 0, 4, 2	−0.2149	−0.2164	0.0156
19f, 0, 4, 2	−0.1827	−0.1843	0.0136
15f, 0, 4, 3	−0.0675	−0.3387	−0.0124
16f, 0, 4, 3[a]	−0.0556	−0.2797	0.0359
17f, 0, 4, 3	−0.0464	−0.2336	0.0159
18f, 0, 4, 3	−0.0391	−0.1971	0.0109

[a]Perturbed state for which the long-range model may not be valid. This state was excluded from calculations of the average $V_{\mathrm{ion}}(2p)$ and $\Delta E(2p \leftarrow X)$.

By combining Eqs. (3) and (4) and using the appropriate groups of $\Delta E(3d \leftarrow 2p)$ and $\Delta E(nf \leftarrow 3d)$ values, one may obtain the energy levels of the $2p$ states, $\Delta E(2p \leftarrow X)$. Just as for the calculation of $V_{\mathrm{ion}}(2p)$, each different nf state yields a different value for $\Delta E(2p \leftarrow X)$. These values are all within 0.025 cm^{-1} of each other, indicative of the sum of errors in the model calculation $E_{\mathrm{quad,pol}}$ and the ionization potential of H_2, $V_{\mathrm{ion}}(H_2)$. We average the $\Delta E(2p \leftarrow X)$ values obtained from transitions emanating from a particular $2p$ state to obtain the average $\Delta E(2p \leftarrow X)$. These derived model-dependent [3] values are given in column 2 of Table VI. Once $\Delta E(2p \leftarrow X)$ is known, then the model-dependent absolute energy levels (term values) of the $3d$ and nf states we have measured can be obtained by adding the transitions energies of Tables IV and V to the term values of Table VI, column 2.

The theoretical intervals in the third column of Table V are obtained from a rearrangement of Eqs. (3) and (4), which is

$$\Delta E(nf \leftarrow 3d) = V_{\mathrm{ion}}(H_2) - \mathscr{R}/n^2 + E_{\mathrm{quad,pol}} + E(R) - \Delta E(2p \leftarrow X) - \Delta E(3d \leftarrow 2p), \tag{5}$$

TABLE IV. Transition energies from $2p$ metastable states to $3d$ intermediate states.

Transition	Interval (cm^{-1})
$3d\ ^3\Sigma$, $v=0$, $N=1$, $J=2 \leftarrow 2p\ ^3\Pi$, $v=0$, $N=1$ $J=2$ (ortho)	16 854.8915(20)
$3d\ ^3\Sigma$, $v=0$, $N=2$, $J=3 \leftarrow 2p\ ^3\Pi$, $v=0$, $N=2$ $J=3$ (para)	16 764.1639(20)
$3d\ ^3\Sigma$, $v=0$, $N=3$, $J=4 \leftarrow 2p\ ^3\Pi$, $v=0$, $N=3$ $J=4$ (ortho)	16 654.2712(50)
$3d\ ^3\Pi$, $v=0$, $N=1$, $J=2 \leftarrow 2p\ ^3\Pi$, $v=0$, $N=1$ $J=2$ (ortho)	17 212.0622(20)
$3d\ ^3\Pi$, $v=0$, $N=2$, $J=3 \leftarrow 2p\ ^3\Pi$, $v=0$, $N=1$ $J=2$ (ortho)	17 199.2420(20)
$3d\ ^3\Pi$, $v=0$, $N=3$, $J=4 \leftarrow 2p\ ^3\Pi$, $v=0$, $N=2$ $J=3$ (para)	17 202.5479(20)
$3d\ ^3\Pi$, $v=0$, $N=3$, $J=4 \leftarrow 2p\ ^3\Pi$, $v=0$, $N=3$ $J=4$ (ortho)	17 261.3278(30)
$3d\ ^3\Delta$, $v=0$, $N=3$, $J=4 \leftarrow 2p\ ^3\Pi$, $v=0$, $N=3$ $J=4$ (ortho)	17 537.0313(100)

TABLE V. List of nf Rydberg levels showing the measured and theoretical intervals between nf Rydberg and $3d$ intermediate levels and the difference between measured and theoretical intervals. All units are cm^{-1}.

Rydberg state label nL, v, R, N	Measured $\Delta E(nf \leftarrow 3d)$	Theoretical $\Delta E(nf \leftarrow 3d)$	Difference [(Expt.) −(Theor.)]
$2p\ ^3\Pi$, $v=0$, $N=2 \rightarrow 3d\ ^3\Sigma$, $v=0$, $N=2 \rightarrow$			
25f, 0, 2, 2	12 589.6296(20)	12 589.6263	0.0033
26f, 0, 2, 2	12 602.8786(30)	12 602.8772	0.0014
25f, 0, 2, 3	12 589.7257(20)	12 589.7307	−0.0050
26f, 0, 2, 3	12 602.9577(20)	12 602.9625	−0.0048
$2p\ ^3\Pi$, $v=0$, $N=2 \rightarrow 3d\ ^3\Pi$, $v=0$, $N=3 \rightarrow$			
25f, 0, 2, 4	12 151.3629(20)	12 151.3604	0.0025
26f, 0, 2, 4	12 164.5855(20)	12 164.5849	0.0006
27f, 0, 2, 4	12 176.4189(30)	12 176.4106	0.0083
28f, 0, 2, 4	12 186.9690(30)	12 186.9608	0.0082
29f, 0, 2, 4	12 196.4436(30)	12 196.4421	0.0015
$2p\ ^3\Pi$, $v=0$, $N=1 \rightarrow 3d\ ^3\Pi$, $v=0$, $N=2 \rightarrow$			
20f, 0, 3, 1	12 349.1713(20)	12 349.1762	−0.0049
20f, 0, 3, 2	12 349.3129(20)	12 349.3090	0.0039
20f, 0, 3, 3	12 349.4655(20)	12 349.4640	0.0015
21f, 0, 3, 1	12 374.7204(20)	12 374.7250	−0.0046
21f, 0, 3, 2	12 374.8493(20)	12 374.8476	0.0017
21f, 0, 3, 3	12 375.0009(20)	12 375.0054	−0.0045
22 f, 0, 3, 1	12 396.8657(20)	12 396.8678	−0.0021
22 f, 0, 3, 2	12 396.9733(20)	12 396.9681	0.0052
22 f, 0, 3, 3	12 397.0911(30)	12 397.0873	0.0038
$2p\ ^3\Pi$, $v=0$, $N=2 \rightarrow 3d\ ^3\Pi$, $v=0$, $N=3 \rightarrow$			
17f, 0, 4, 2	12 347.9896(30)	12 347.9923	−0.0027
18f, 0, 4, 2	12 389.0742(30)	12 389.0770	−0.0028
19f, 0, 4, 2	12 423.8407(40)	12 423.8437	−0.0030
15f, 0, 4, 3	12 240.0736(20)	12 240.0886	−0.0150
16f, 0, 4, 3[a]	12 298.9532(20)	12 299.2518	−0.2986
17f, 0, 4, 3	12 348.2255(40)	12 348.2212	0.0043
18f, 0, 4, 3	12 389.2705(30)	12 389.2674	0.0031

[a]Perturbed state for which the long-range model may not be valid. This state was excluded from calculations of the average $V_{ion}(2p)$ and $\Delta E(2p \leftarrow X)$.

where all of the terms on the right-hand side are known. As can be seen from the nonzero difference in the last column of Table V, the measurements do not agree well with the theoretical predictions, at least to within the transition measurement error of 0.002 cm^{-1}. If one assumes that the error in the theory is about 0.02 cm^{-1} then there is good agreement. Typical magnitudes of $E_{quad,pol}$ are about 0.2 cm^{-1}, so the model [3] is accurate to about 10%.

By construction, the deviations in the last column of Table V (excluding the anomalous 16f state) average to zero. The deviations of the theoretical predictions from the measured values are apparently random. The deviations are probably due to three factors that the long-range model calculation [3] of $E_{quad,pol}$ ignores. One factor is the effect of the core penetration of the nf wave function. Even for $L=3$ there is still some penetration and thus the perturbation in the energy level will be slightly different from the model prediction, which assumes perturbation from a point quadrupole moment and point polarizability. Finite core penetration is naturally treated in multichannel quantum-defect theory, which is beyond the scope of this experimental paper. Also there are higher-order multipole Coulomb moments that slightly shift the energy level. The third factor is that of spin. The model ignores spin, but the levels have fine-structure splitting of up to 0.03 cm^{-1} and there is no reason to believe that a Rydberg state's energy level is exactly what it would be if spin did not exist.

The values of Table VI represent a correction to two values on page E8 of Crosswhite's compilation of Dieke's term values of H_2 [15]. However, the two pairs of numbers cannot be compared directly since Dieke's values were for the weighted average of the fine-structure components of the $2p$ state. We can easily resolve the fine-structure components and our values are for the energy of a particular N,J,F fine-structure component. The particular values of N,J,F are given in Table VI. The fine structure of the $2p$ states is very well known via the microwave measurements of Lichten and co-workers [27,16], so we can easily calculate the energy of the center of mass of the fine structure relative to the position of the fine-structure component that we measure. The shift is given in column 3 of Table VI. Column 4 is the sum of columns 2 and 3 and is our measurement of the center of mass of the $2p$ states. The numbers in column 4 can be directly compared with Dieke's numbers [15] in column 5. The last column of Table VI is their differences, which are our corrections to Dieke's term values. The correction, a negative number, must be added to Dieke's values to give

TABLE VI. Term values of $\Delta E(2p \leftarrow X)$ measured in this paper and a comparison to Dieke's term values [15]. All units are cm^{-1}. c.m. indicates center of mass.

Rydberg state $2p\ ^3\Pi$, v, N, J, F	$\Delta E(2p \leftarrow X)$ (this paper)	c.m. correction	$\Delta E(2p \leftarrow X)$ c.m. (this paper)	$\Delta E(2p \leftarrow X)$ c.m. (Dieke)	Difference
0, 2, 3, 3 (para)	95 062.314(25)	0.071	95 062.385(25)	95 212.11	−149.725
0, 1, 2, 3 (ortho)	94 941.546(25)	0.062	94 941.608(25)	95 091.32	−149.712

the correct energy level, i.e., the absolute value of the correction must be subtracted from Dieke's values. Averaging the last column of Table VI gives a correction of $-149.718(25)$ cm^{-1}. Averaging this correction with the $-149.689(25)$ cm^{-1} derived from the $v=1$ Rydberg H_2 states in Ref. [2] (updated with the present value of H_2 ionization potential [8,9]) gives a *final correction of* $-149.704(25)$ cm^{-1}. The accuracy obtained by applying this correction to all of the rest of the triplet term values in Dieke's tables depends on the accuracy of Dieke's measurements within the triplet manifold [15]. As we have found in this paper and in Ref. [1], his measurements of four $v=0$ and $v=1$, $2p$ states are accurate relative to each other to within 0.04 cm^{-1}.

V. CONCLUSION

We have measured the autoionization rates of a variety of purely rotationally autoionizing triplet nf, $v=0$, $R\neq 0$ Rydberg states of H_2, using precision single-frequency cw dye lasers crossed with a molecular beam. The rate measurements are accurate to about 20%. The autoionization rates agree well with the predictions of the long-range model, which are based on the interaction of the Rydberg electron with the polarizability and quadrupole moment of the H_2^+ core. However, we have seen some autoionizing states that cannot autoionize according to the model [3]. This is explained by ''forced'' or core-assisted field ionization due to a small stray external electric field and also by the model not including higher-order multipole moments of the core, imperfect quantum numbers, and spin.

We have measured the energies of transitions from certain metastable $2p$, $v=0$ states of H_2 to $3d$ states and then to the Rydberg states, using a wavemeter and I_2 reference lines. These measurements are accurate to 0.002 cm^{-1}, which is 60 MHz. Using an extrapolation of the Rydberg series, we have obtained the ionization potential $V_{\rm ion}(2p)$ of the $2p$ states. Then using the ionization potential of H_2 from a different experiment [8,9] and the long-range Coulomb model [3] energy perturbation, we obtain the vacuum uv interval $\Delta E(2p \leftarrow X)$ between the triplet $2p$ states and the singlet ground state, to an accuracy of 0.025 cm^{-1}. Even though no transition from a singlet to a triplet state has been observed for this paper, we still link the singlet and triplet manifolds with very high precision. This method links the manifolds at the ionization potential, where the singlet-triplet distinction vanishes as one electron is removed to infinity.

We have updated the correction to Dieke's triplet term values [15]. The present correction is $-149.704(25)$ cm^{-1}. Jungen *et al.* [14], using a completely different Fourier spectroscopy method and different $v=0$ H_2 states, obtain a correction of $-149.700(50)$ cm^{-1}, showing that their measurements are in excellent agreement with ours.

ACKNOWLEDGMENTS

We thank E. E. Eyler for his computer programs that calculated the $E_{\rm quad,pol}$ values. We thank J. R. Lawall for the use of the wavemeter.

[1] M. D. Lindsay, A. W. Kam, J. R. Lawall, P. Zhao, F. M. Pipkin, and E. E. Eyler, Phys. Rev. A **41**, 4974 (1990). (See also Ref. [2].)

[2] M. D. Lindsay, Ph.D. thesis, Harvard University, 1990 (unpublished). Contains measurements of $v=1$ states [1] and $v=0$ states (this paper). The thesis contains summary values of the $v=1$ states that differ slightly from those of Ref. [1], due to the fact that more $v=1$ states were measured for the thesis. This paper contains summary values for $v=1$ states that differ slightly from those of the thesis, since there is now a slightly different value for $V_{\rm ion}(H_2)$.

[3] E. E. Eyler, Phys. Rev. A **34**, 2881 (1986).

[4] C. Jungen, I. Dabrowski, G. Herzberg, and M. Vervloet, J. Chem. Phys. **93**, 2289 (1990).

[5] P. W. Arcuni, Z. W. Fu, and S. R. Lundeen, Phys. Rev. A **42**, 6950 (1990).

[6] P. B. Davies, M. A. Guest, and R. J. Stickland, J. Chem. Phys. **93**, 5408 (1990).

[7] W. G. Sturrus, E. A. Hessels, P. W. Arcuni, and S. R. Lundeen, Phys. Rev. A **44**, 3032 (1991).

[8] J. M. Gilligan and E. E. Eyler, Phys. Rev. A **46**, 3676 (1992).

[9] D. Shiner, J. M. Gilligan, B. M. Cook, and W. Lichten, Phys. Rev. A **47**, 4042 (1993).

[10] W. L. Glab. K. Qin, and M. Bistransin, J. Chem. Phys. **102**, 2338 (1995).

[11] S. Kim and E. Mazur, Phys. Rev. A **52**, 992 (1995).

[12] E. McCormack, J. M. Gilligan, C. Cornaggia, and E. E. Eyler, Phys. Rev. A **39**, 2260 (1989).

[13] J. T. Hougen, *The Calculation of Rotational Energy Levels and Rotational Line Intensities in Diamotic Molecules*, Natl. Bur. Stand. (U.S.) Monograph 115 (U.S. GPO, Washington, DC, 1970).

[14] William Lichten, Phys. Rev. **120**, 848 (1960); **126**, 1020 (1962).

[15] Crosswhite's compendium of Dieke's results: H. M. Cross-

white, *The Hydrogen Molecule Wavelength Tables of Gerhard Heinrich Dieke* (Wiley-Interscience, New York, 1972).

[16] W. Lichten, T. Wik, and Terry A. Miller, J. Chem. Phys. **71**, 2441 (1979).

[17] T. R. Wik, Ph.D. thesis, Yale University, 1977 (unpublished).

[18] G. R. Janik, O. C. Mullins, C. R. Mahon, and T. F. Gallagher, Phys. Rev. A **35**, 2345 (1987).

[19] E. Y. Xu, H. Helm, and R. Kachru, Phys. Rev. A **38**, 1666 (1988).

[20] R. D. Knight, J. E. Sohl, Y. Zhu, and L.-G. Wang, in *Proceedings of the Conference on Laser Spectroscopy VIII, Are, Sweden, 1987*, edited by W. Persson and S. Svanberg, Springer Series in Optical Sciences Vol. 55 (Springer-Verlag, New York, 1987), p. 198.

[21] M. G. Littman, M. M. Kash, and D. Kleppner, Phys. Rev. Lett. **41**, 103 (1978).

[22] S. Gerstenkorn and P. Luc, *Atlas du Spectre D'Absorption de la Molecule d'Iode: 14 800–20 000 cm^{-1}* (CNRS, Paris, 1978). A systematic correction to this reference is described by S. Gerstenkorn and P. Luc, Rev. Phys. Appl. **14**, 791 (1979).

[23] S. Gerstkenkorn, J. Verges, and G. Chevillard, *Atlas du Spectra d'Absorption de la Molecule d'Iode: 11 000 cm^{-1}–14 000 cm^{-1}* (Laboratoire Aimé-Cotton, CNRS II, Orsay, 1982).

[24] J. L. Hall and S. A. Lee, Appl. Phys. Lett. **29**, 367 (1976); T. Baer, R. V. Kowalski, and J. L. Hall, Appl. Opt. **19**, 3173 (1980).

[25] David M. Bishop and Lap M. Cheung, Phys. Rev. A **16**, 640 (1977); G. Hunter, A. W. Yau, and H. O. Pritchard, At. Data Nucl. Data Tables **14**, 11 (1974).

[26] $E(R)$ was denoted $E(v,R)$ in Ref. [1] but for this paper $v=0$ for all states, so the v is dropped.

[27] W. Lichten and T. Wik, J. Chem. Phys. **69**, 5428 (1978).